

2010-02-06

# Converting shear probe, thermistors and micro-conductivity signals into physical units

Rolf Lueck

## Introduction

For quantitative scientific interpretation, the signals produced by shear probes, thermistors and micro-conductivity probes must be converted into physical units. This note explains how to use the shear probe calibration, electronics calibration and other information to produce signals in physical units.

## Table of Contents

Converting shear probe, thermistors and micro-conductivity signals into physical units.....	1
Introduction .....	1
Shear probe fundamentals.....	1
Shear Probe Amplifier .....	3
Analog-to-Digital Conversion .....	6
Wavenumber Response of Shear Probes .....	6
Water Density Effects.....	6
Thermistor Circuits.....	6
Temperature De-convolution.....	9
Temperature gradient using first difference.....	9
Temperature gradient using a high-pass filter .....	10
Micro-conductivity probe fundamentals.....	11
Using Micro-conductivity calibration report .....	12
Micro-conductivity De-convolution .....	13
References .....	14

## Shear probe fundamentals

The shear probe, also frequently called the “air-foil” probe, was conceived by H. S. Ribner and T. Siddon at the University of Toronto (Siddon and Ribner 1965). It was adapted for use in water by T. Osborn who first used it in the ocean in 1972 (Osborn 1974). Since then, it has become the standard sensor for measuring oceanic turbulence at dissipation scales.

The shear probe consists of a piezo-ceramic bender that is mounted into the end of a stainless steel sting with about one half of the length of the bender protruding outward (Figure 1). The bender produces a charge in response to a bending force. In the frequency range of oceanic turbulence (1 – 100 Hz), the impedance of the ceramic is extremely high (~1GΩ). RSI uses a proprietary Teflon isolation to block moisture from reaching the bender. A soft and pliable silicone-rubber covers the assembly in an axial-symmetric form. The shape of the probe tip is similar to a bullet.

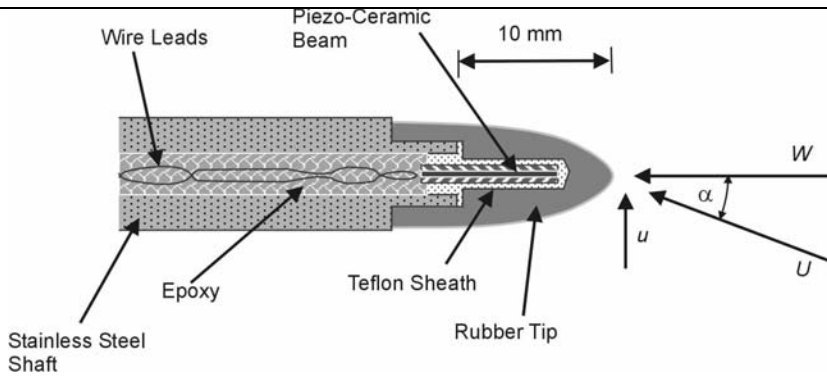


Figure 1: Sketch of shear probe and velocity vectors.

The bender is 1.5 mm wide and 0.5 mm thick. It bends far more easily in its thin direction than in the other direction. (This is somewhat like a diving board at a pool which bends easily in one direction but not the other.) Thus, the shear probe responds only to the component of velocity perpendicular to the broad side of the bender (the  $u$  component indicated in Figure 1). A flat surface is milled into the side of the shear probe body and this flat is parallel to the broad side of the bender. The flat is used to orient the probes when they are being mounted into their holders on the front of an instrument. To measure two orthogonal components of velocity fluctuations ( $u$  and  $v$ ), two probes must be installed side-by-side with their sensitive axes oriented at  $90^\circ$  to each other.

The shear probe responds linearly to cross-stream velocity fluctuations when the angle of attack,  $\alpha$ , is small. A velocity component orthogonal to the axis of the probe produces a pressure difference across the tip of the probe and this forces a small bending of the beam. A detailed discussion can be found in Osborn and Crawford (1980). Bending the beam produces a charge given by

$$Q_p = \sqrt{2}\hat{S}U^2 \sin(2\alpha) = 2\sqrt{2}\hat{S}U \cos(\alpha)U \sin(\alpha) = 2\sqrt{2}\hat{S}Wu \quad (1)$$

where  $U$  is the total velocity vector,  $W$  is the velocity along the axis of the probe,  $u$  is the velocity orthogonal to the axis of the probe (and aligned with the sensitive axis of the ceramic), and  $\hat{S}$  is the sensitivity of the probe (Figure 1). The factor of  $2\sqrt{2}$  is an artifact of the method of calibration. Typical sensitivities are in the range of  $\hat{S} = (0.05 - 0.10) \times 10^{-9} \text{ C/m}^2\text{s}^{-2}$ . This value is slightly temperature dependent and increases with increasing temperature.

There are two ways to capture the signal produced by a shear probe — a charge-transfer amplifier and a high-impedance buffer amplifier. Calibrations can be made with either type of amplifier with the calibration facility at RSI. All instruments produced by RSI use a charge-transfer amplifier. With a charge transfer amplifier, the charge produced by the shear probes is continuously removed and transferred to a feed-back capacitor of known value and exceptional temperature and aging stability ( $1 \times 10^{-4} \text{ }^\circ\text{C}^{-1}$ ). The output voltage of the charge-transfer amplifier is the probe charge divided by the feed-back capacitance, namely

$$E_I = \frac{Q_p}{C_I} = \frac{2\sqrt{2}\hat{S}Wu}{C_I} \quad (2)$$

where the subscript  $I$  refers to the amplifier in an instrument. The voltage across the shear probe is always held at zero. Thus, the lead capacitance of the connection between the shear probe and the amplifier does not effect the output given in equation (2).

The shear probe is calibrated by rotating it at 1 Hz in a water jet of known flow and by varying the angle of attack of the jet with respect to the axis of the probe (Osborn and Crawford 1980). The signal produced by the probe is sinusoidal and has a frequency of 1 Hz. We measure the rms voltage of the output of the charge-transfer amplifier. This rms voltage divided by the speed squared is then regressed against  $\sin(2\alpha)$  to derive the sensitivity of the probes. The sensitivity is the slope of the best fit of

$$\frac{E_C^{rms}}{U^2} \text{ versus } \sin(2\alpha).$$

Using the rms voltage rather than the peak voltage accounts for the factor of  $\sqrt{2}$  in equation (1). The capacitor used in the charge-transfer amplifier in the calibrator has a value of  $C_C = 1.500 \text{ nF} \pm 0.5\%$ . Thus, the peak voltage produced by the probe in the calibrator is

$$E_C = \frac{Q_P}{C_C} = \frac{\sqrt{2}\hat{S}U^2}{C_C} \sin(2\alpha) = \frac{2\sqrt{2}\hat{S}Wu}{C_C} = 2\sqrt{2}SWu \quad (3)$$

where the subscripts refer to the calibrator and we have defined

$$S = \frac{\hat{S}}{C_C}. \quad (4)$$

The value  $S$  is provided with the calibration certificate and typically falls in the range of

$$S = 0.05 - 0.10 \frac{\text{V}}{\text{m}^2\text{s}^{-2}}.$$

The feed-back capacitor in instruments manufactured by RSI is usually  $C_I = 1.50 \text{ nF} \pm 2\%$ . The temperature coefficient of this capacitor is less than  $1 \times 10^{-4} \text{ }^\circ\text{C}^{-1}$ . Other feedback capacitance is available on request. A smaller capacitor will increase the output level while a larger one will decrease the output level. The voltage produced by the charge-transfer amplifier in the instrument is

$$E_I = \frac{2\sqrt{2}\hat{S}Wu}{C_I} = \frac{C_C}{C_I} 2\sqrt{2}SWu \quad (5)$$

where the subscripts  $I$  and  $C$  refer to the instrument and the calibrator, respectively, and using equation (4). Most instruments are designed to have  $C_C / C_I = 1$ .

An alternative method of capturing the output of the shear probe is to connect it to a very high-impedance (100 G $\Omega$ ) voltage buffer. The charge produced in response to the bending of the beam produces a voltage because the probe has a capacitance of approximately 1 nF. The capacitance of the probes is temperature dependent. Thus, even if the charge produced per unit of mechanical excitation were independent of temperature, the voltage produced by the probes will still be temperature dependent. In addition, the lead capacitance must be accounted for in both the calibrator and in the instrument. The lead capacitance adds to the probe capacitance and reduces the output voltage. Most co-axial cables have a capacitance of 100 pF per meter.

The output voltage from the probe calibrator using a voltage buffer is

$$E_p = \sqrt{2}SU^2 \sin(2\alpha) = 2\sqrt{2}SU \cos(\alpha)U \sin(\alpha) = 2\sqrt{2}SWu \quad (6)$$

where the symbols are as before.

### Shear Probe Amplifier

The front-end component of the shear probe circuit in an instrument is the charge-transfer amplifier discussed above. A block diagram is shown in Figure 2. The next stage is a time-differentiator that produces an output proportional to the rate of change of voltage (produced by the charge-transfer front end). The gain of a differentiator increases in proportion to frequency. Stability requires that the gain be reduced above a certain frequency. The last stage of the shear amplifier is a broad-band gain which is selectable with one resistor. Usually, this gain is set to unity.

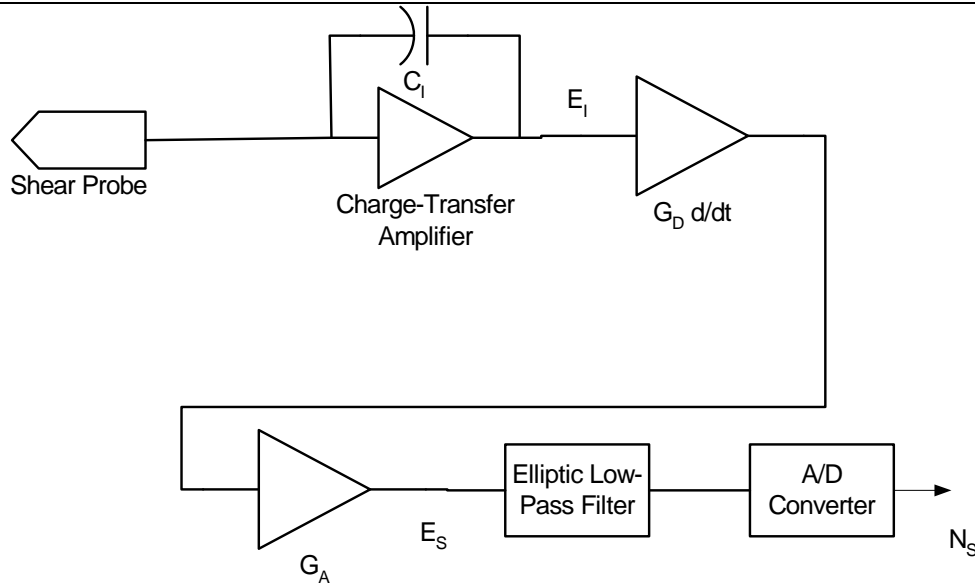


Figure 2. Block diagram of the shear probe electronics on a typical instrument.

The output from the shear probe circuit is

$$\begin{aligned}
 E_S &= \frac{C_C}{C_I} 2\sqrt{2}G_D G_A S W \frac{\partial u}{\partial t} = \frac{C_C}{C_I} 2\sqrt{2}G_D G_A S W^2 \frac{\partial u}{\partial z} \\
 &= 2\sqrt{2}G S W^2 \frac{\partial u}{\partial z}
 \end{aligned} \tag{7}$$

where  $G_D(f)$  is the gain of the differentiator relative to that of an ideal differentiator (which has a gain of  $j2\pi f$ ) and  $G_A$  is the gain of the broad-band amplifier after the differentiator. The “frozen field” assumption is used to convert time derivatives into spatial derivatives, namely

$$\frac{\partial}{\partial z} = \frac{1}{W} \frac{\partial}{\partial t} \tag{8}$$

Here the co-ordinate  $z$  refers to the direction of travel of the probes which must also be the direction of the axis of the probes. On a vertical profiler  $z$  would be nominally vertical while on a horizontal profiler  $z$  is a direction in the horizontal plane. All gain stages in equation (7) can be combined into a single parameter

$$G = \frac{C_C}{C_I} G_D G_A \tag{9}$$

This gain is provided by the frequency response calibration of the electronics. A certificate of frequency response calibration between 0.05 and 200 Hz is provided with each instrument (Figure 3 and Figure 4). The calibration should be repeated at regular intervals, because aging circuit components (in particular capacitors) affect the frequency response of the circuit.

The shear probe circuits are calibrated by coupling a pseudo-random voltage into the charge-transfer amplifier via a 1.500 nF capacitor. The output is taken from the test point near the analog bus connector on the analog (ASTP) board. The contribution from the anti-aliasing filter (usually set for 165 Hz) is not included in the calibration (Figure 2). The user needs only the single factor  $G$  to convert the voltage output into a shear signal with equation (7). The factor of  $G$  has units of seconds.

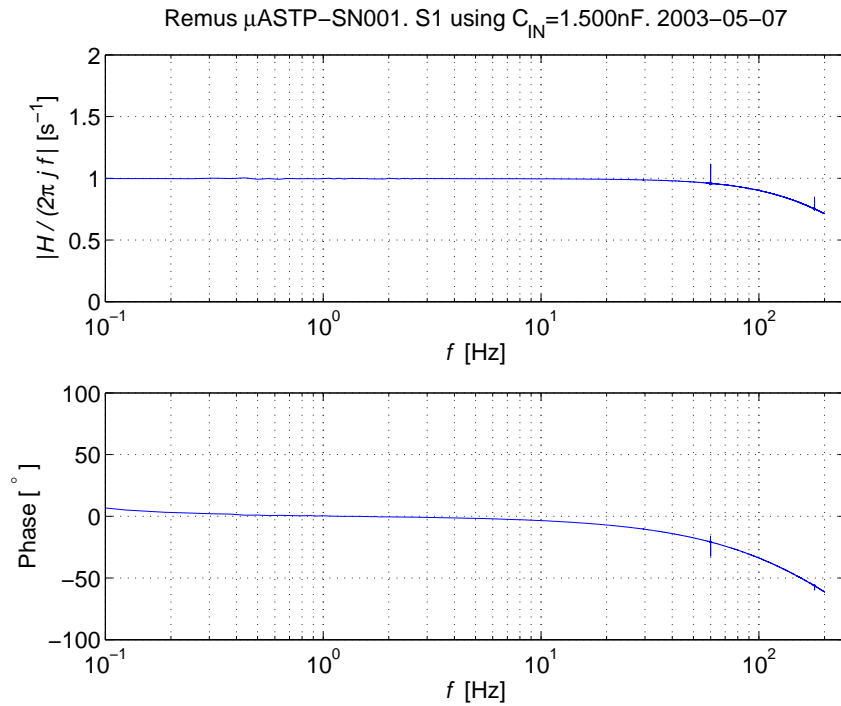


Figure 3. An example of the frequency response calibration of the shear probe circuit.

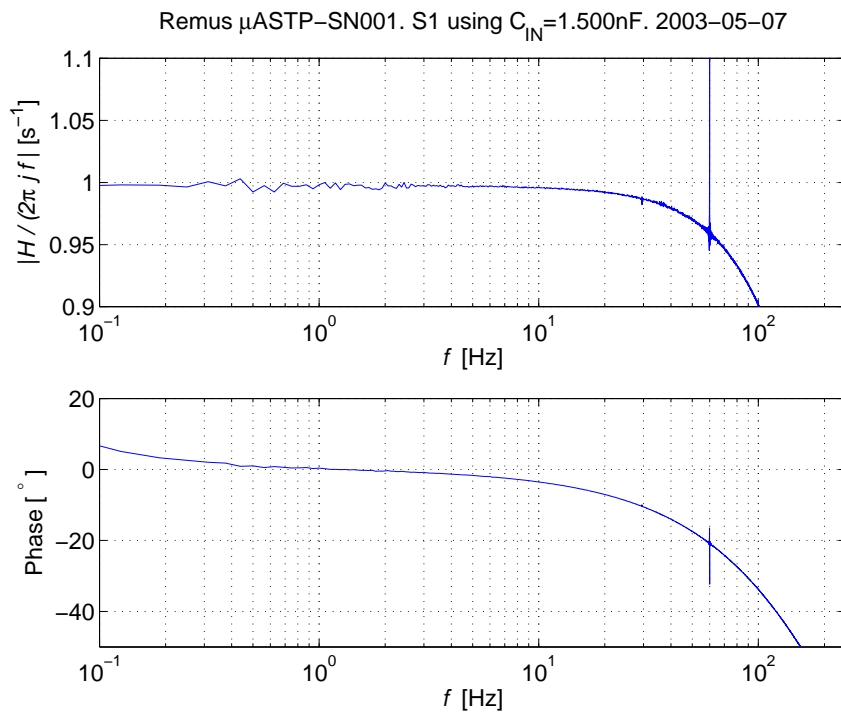


Figure 4. An example of the frequency response calibration of a shear probe circuit. Zoom-in view. The combined gain of the electronics and the feedback capacitors is within 10% of unity all the way to 100 Hz. The gain factor  $G$  of equation (8) is within 1% of unity.

## Analog-to-Digital Conversion

The analog to digital converter in instruments manufactured by RSI usually has a full-scale range of  $\pm 2.5V$  and a resolution of 16 bits. The relationship between the 2-byte binary number produced by the A/D converter and the signal voltage is then

$$N_s = \frac{2^{16}}{5} E_s. \quad (10)$$

Using equations (7) and (10), the relationship between the 2-byte number and the shear is

$$N_s = \frac{2^{16}}{5} 2\sqrt{2}SGW^2 \frac{\partial u}{\partial z}. \quad (11)$$

## Wavenumber Response of Shear Probes

The shear probes produced by RSI smooth spatial structures with scales comparable to and smaller than the diameter of the probe. This spatial averaging has been examined by Macoun and Lueck (2004) who recommend using a spectral correction factor of

$$\Phi(k) = 1 + (k/50)^2 \quad (12)$$

where  $k$  is the wavenumber in cycles per meter [cpm] and 50 cpm represents the half-power wavenumber of the shear probe.

## Water Density Effects

The bending force on the shear probe is proportional to the dynamic pressure,  $\rho U^2$ . The shear probes are usually calibrated at room temperature (20-25°C) in fresh water which has a density of  $\rho = 997 - 998 \text{ kg m}^{-3}$  and is about 2 to 3 percent less dense than typical seawater. Users may scale up the sensitivity,  $S$ , according to the *in situ* density.

## Thermistor Circuits

A typical circuit block diagram for the FP07 thermistor consists of a bridge amplifier, a differentiator and a summing amplifier (Figure 5). The main voltage output is  $E_{T\_dT}$  which is the analog sum of the amplified bridge voltage,  $E_T$ , and its time derivative. The main sampling output is  $N_{T\_dT}$ . This is usually called the “pre-emphasized” temperature signal. The gain  $G_D$  is very close to unity and its exact value is provided in the circuit calibration certificate. For low frequencies,  $f < (2\pi G_D)^{-1}$ , the signal is mainly temperature while for high frequencies,  $f > (2\pi G_D)^{-1}$ , the signal is mainly the derivative of temperature. This technique improves the signal-to-noise ratio of temperature measurements by 4 to 5 orders of magnitude. It is discussed fully in Mudge and Lueck (1994) which is also available as RSI Application Note AN-002.

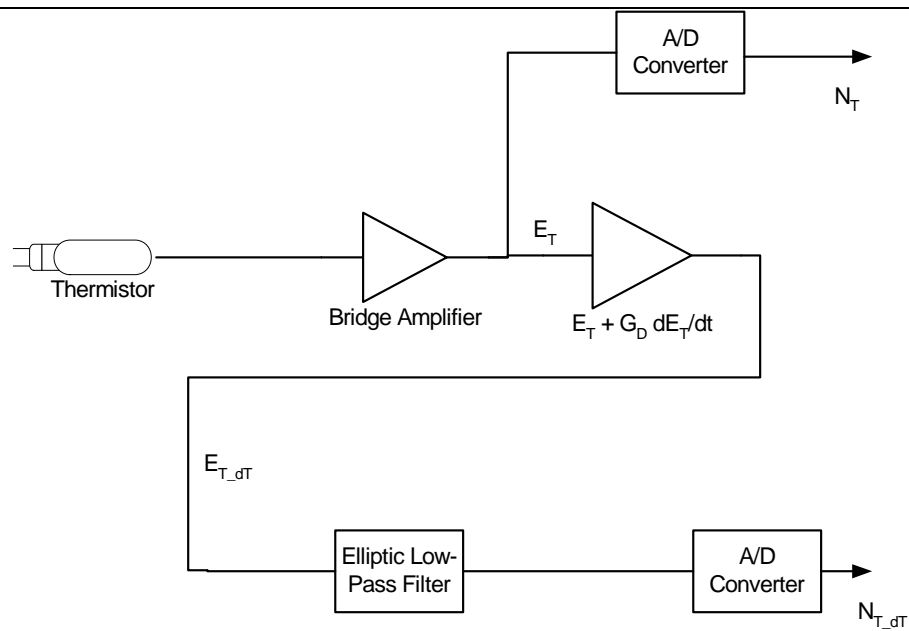


Figure 5. Block diagram of typical thermistor circuit. There are two outputs. One,  $N_T$ , is approximately linear in temperature. The other output,  $N_{T,dT}$ , is a pre-emphasized signal that consists of the analog sum of the bridge signal and its time derivative.

The transfer function of the thermistor electronics is calibrated by inputting a pseudo-random voltage into the bridge and monitoring the output of the low-pass elliptic anti-aliasing filter. The transfer function, relative to that of an ideal differentiator is provided in the calibration certificate (Figure 6 and Figure 7). The gain between 2 and 20 Hz is used to estimate  $G_D$ .

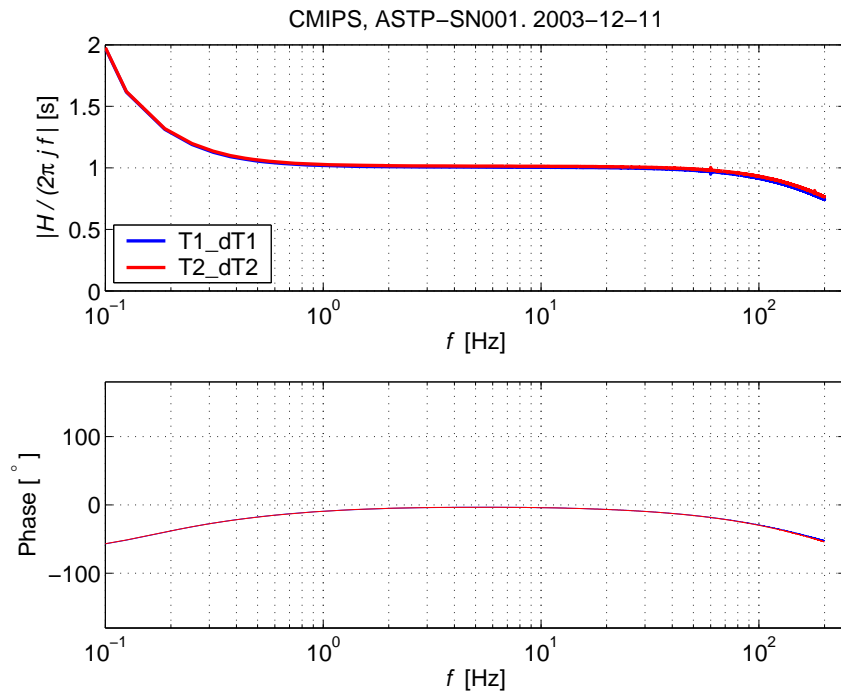


Figure 6. Example of a frequency response calibration of the thermistor circuit in a typical instrument.

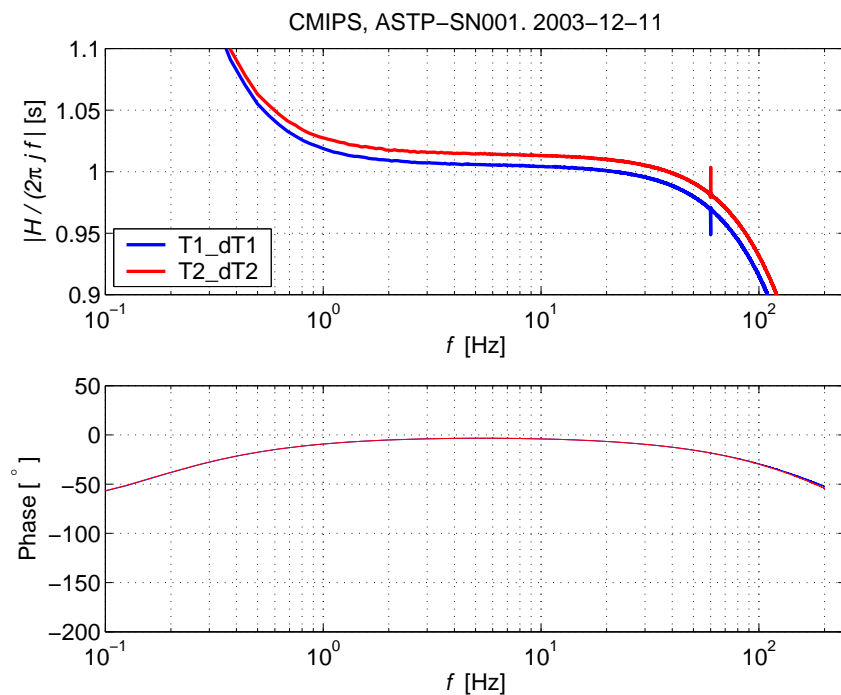


Figure 7. Example of a frequency response calibration of the thermistor circuit in a typical instrument. Zoom-in view. The gain of channel 1 is 1.00 seconds while the gain of channel 2 is 1.01 seconds.

The other output of the thermistor circuit is the amplified bridge voltage,  $E_T$ , and its sampled version,  $N_T$ . It is provided for users who wish to sample the thermistor signal directly, without resolution enhancing pre-

emphasis. No anti-aliasing filtering is applied to  $E_T$ . This signal can also be used to evaluate the success of the deconvolution of the pre-emphasized signal.

### Temperature De-convolution

The pre-emphasized signal is neither proportional to temperature nor to its derivative. This signal must be deconvolved to obtain a signal related to temperature or to its derivative. The procedure is described in detail in Mudge and Lueck (1994), also available as RSI Application Note AN-002. To derive a high-resolution temperature signal  $N_{\hat{T}}$ , the pre-emphasized signal,  $N_{T\_dT}$ , is low-pass filtered with a first-order Butterworth filter with a cut-off frequency of

$$f_c = \frac{1}{2\pi G_D} \text{ [Hz]} \quad (13)$$

where  $G_D$  is the gain of the differentiator relative to that of an ideal differentiator. This gain is usually within one or two percent of unity (Figure 7). The de-convolution process is depicted in Figure 8.

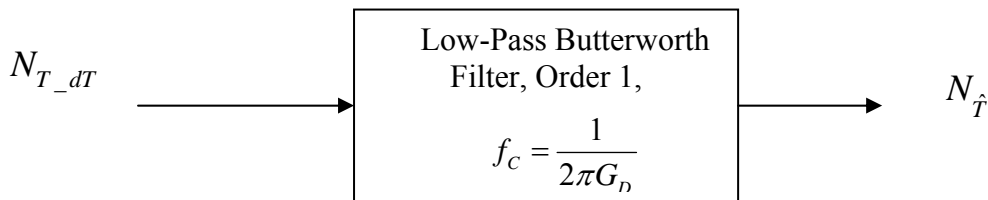


Figure 8. Block diagram of the de-convolution process.

The de-convolved signal will resolve oceanic temperature fluctuations down to about  $10\mu^{\circ}\text{C}$ . The de-convolved signal must be converted to physical units by a polynomial regression against an accurate and concurrent measurement of temperature with another instrument, such as the SeaBird SBE3 thermometer, which is available for all instruments manufactured by RSI. If the temperature span is less than 4 degrees Celsius, a linear regression suffices. For a  $25^{\circ}\text{C}$  and larger span, the regression should be 4<sup>th</sup> order. Regression against an accurate and concurrent temperature measurement will give the following polynomial relationship,

$$\hat{T} = a_0 + a_1 N_{\hat{T}} + a_2 N_{\hat{T}}^2 + a_3 N_{\hat{T}}^3 + a_4 N_{\hat{T}}^4. \quad (14)$$

### Temperature gradient using first difference

There are two ways to derive the temperature gradient signal from the pre-emphasized temperature measurements. The first, more easily implemented, method is to compute the first difference of the high-resolution (and de-convolved) temperature signal  $\hat{T}$  in equation (14). Multiplying this first difference by the sampling rate gives an estimate of the time derivative of temperature. The problem with this method is that a first-difference is only a good approximation to a derivative for frequencies smaller than one-third of the Nyquist frequency (about 80 Hz). Because the frequency response of the FP07 thermistor is not much better than 25 Hz, this first differencing approach might be acceptable. If the main objective of the signal processing is to obtain temperature spectra, this approach is advisable because the spectra can be corrected for the actual transfer function of a first difference operation relative to an ideal derivative. For example, the first difference operation

$$\hat{T}_{\Delta}(n) = (\hat{T}(n) - \hat{T}(n-1)) f_s \quad (15)$$

where  $f_s$  is the sampling rate, and this difference operation has the transfer function of

$$H_{\Delta} = 4f_N \exp\left(j\frac{\pi}{2}\left(1 - \frac{f}{f_N}\right)\right) \sin\left(\frac{\pi}{2} \frac{f}{f_N}\right) \quad (16)$$

where the complex exponential is just a phase factor. The transfer function of a first derivative is  $H_d = j2\pi f$ , so the response of a first difference relative to a first derivative is

$$\frac{H_{\Delta}}{H_d} = 4f_N \exp\left(j\frac{\pi}{2} \frac{f}{f_N}\right) \frac{\sin\left(\frac{\pi}{2} \frac{f}{f_N}\right)}{2\pi f}, \text{ and} \quad (17)$$

$$\frac{H_{\Delta}}{H_d} \approx 1 \text{ for } \frac{f}{f_N} \ll 1$$

Therefore, spectra of the first difference of temperature can be corrected for all frequencies up to and including the Nyquist frequency using equation (17).

The temperature gradient is derived by dividing the estimated temperature derivative by the speed of profiling, that is,

$$\frac{\partial T}{\partial z} = \frac{1}{W} \frac{\partial T}{\partial t}, \quad (18)$$

where  $W$  is the speed of profiling and  $z$  is the direction of travel.

### Temperature gradient using a high-pass filter

The second method for deriving the derivative of temperature is by high-pass filtering the pre-emphasized signal (Figure 9). This removes the temperature portion and leaves the derivative, if the cut-off frequency is as given in equation (13). The high-resolution temperature,  $\hat{T}$ , must still be derived in order to determine the scaling coefficients for the temperature derivative.

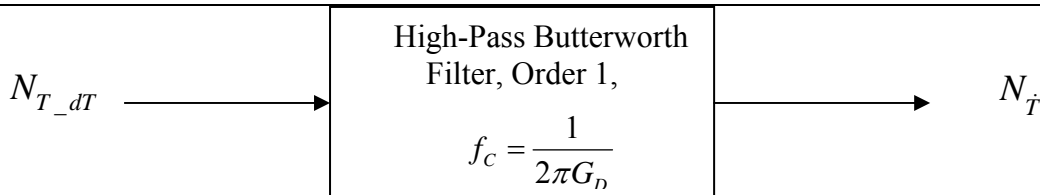


Figure 9. Block diagram for obtaining the temperature gradient from the sampled pre-emphasized signal.

Let  $N_{\dot{T}}$  be the output of the high-pass filtering of the pre-emphasized signal. Then, for low-frequencies,

$$N_{\dot{T}} = G_D \frac{\partial N_{\hat{T}}}{\partial t}. \quad (19)$$

Differentiation of equation (14) gives

$$\frac{\partial \hat{T}}{\partial t} = \left(a_1 + 2a_2 N_{\hat{T}} + 3a_3 N_{\hat{T}}^2 + 4a_4 N_{\hat{T}}^3\right) \frac{\partial N_{\hat{T}}}{\partial t}. \quad (20)$$

Therefore, the high-resolution temperature derivative is

$$\frac{\partial T}{\partial t} = \left(a_1 + 2a_2 N_{\hat{T}} + 3a_3 N_{\hat{T}}^2 + 4a_4 N_{\hat{T}}^3\right) \frac{N_{\dot{T}}}{G_D} \quad (21)$$

where the term in braces is the scale factor that converts the high-pass filtered output into physical units. The scale factor varies only slightly with temperature because the high order coefficients are small compared to the leading linear coefficient  $a_1$ . Note that the term in braces involves  $N_{\hat{f}}$  which is the result of low-pass filtering the pre-emphasized temperature signal while  $N_{\hat{f}}$  is derived by high-pass filtering the pre-emphasized signal.

The temperature gradient is obtained by dividing the temperature derivative by the speed of profiling.

### Micro-conductivity probe fundamentals

The micro-conductivity probe senses the electrical conductivity of seawater by measuring the conductance between two electrodes. In the case of a Sea-Bird SBE7 probe, these electrodes are a pair of identical cylinders (needles) which have one face exposed to seawater and their side (circumference) insulated from the seawater. The faces are coated with platinum black to improve the electrical contact with seawater. The conductance of the path between the electrodes is proportional to the conductivity of the fluid and the area of the surface of the electrodes and inversely proportional to the separation of the electrodes. The surface area of the electrodes does not vary much between different probes because they are made from rods. However, the separation between the electrodes does vary a little because these are hand-placed into position. Thus, for a given fluid conductivity, the conductance of the probes can vary slightly.

The nominal conductance of the SBE7 probes is the inverse of  $R_p=268 \Omega$  in seawater with a conductivity of  $\sigma = 30 \text{ mS cm}^{-1}$ . This will vary by about 10% between probes and will decrease if dirt and plankton cover the surface of the electrodes. Resistance is measured in ohms ( $\Omega$ ), conductance is its inverse and is measured in units of siemens (S) and conductivity is a specific property that is properly given in units of  $\text{S m}^{-1}$ , but oceanographers seem to prefer using  $\text{mS cm}^{-1}$ , and limnologists covet the unit of  $\mu\text{S cm}^{-1}$ .

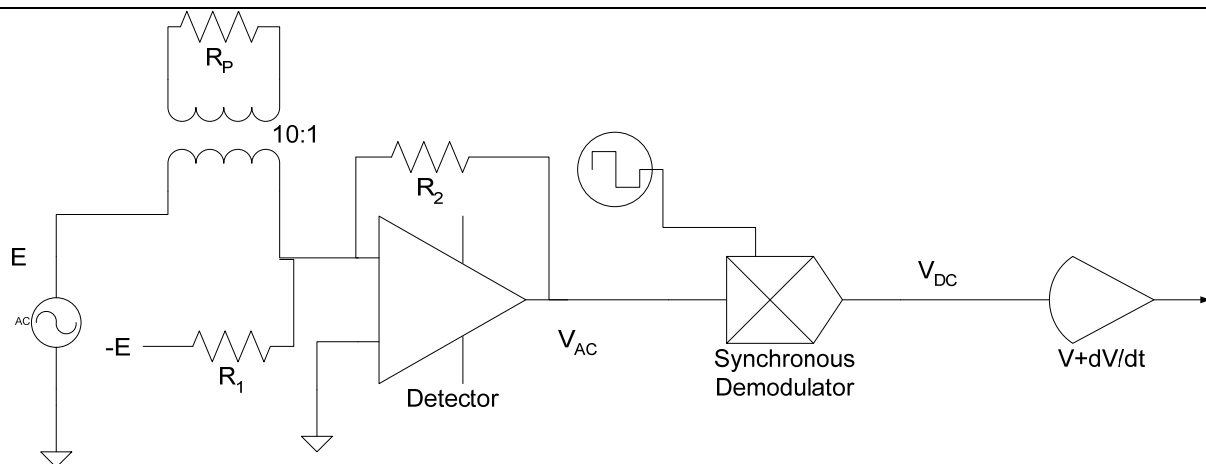


Figure 8. Electrical representation of the micro-conductivity probe and circuit. E is an alternating voltage source used to drive a current through the conductivity probe represented by  $R_p$ . The current is converted into a voltage,  $V_{AC}$ , and is then synchronously demodulated by flipping its phase every half cycle to produce a “DC” signal proportional to the probe current. This signal is pre-emphasized using the usual signal-plus-derivative technique..

A simplified schematic of the micro-conductivity circuit is shown in Figure 8. A constant-amplitude ( $1.1V_{\text{rms}}$ ) voltage of nominal frequency 8kHz is used to drive a current through the conductivity probe. This current is proportional to the conductance of the probe (and, hence the conductivity of the fluid) and is converted into a voltage by the detector amplifier. A transformer with a winding ratio of 10-to-1 is used to galvanically isolate the probe so that all current is constrained to a path between the electrodes. In addition, the transformer makes the effective resistance of the probe 100 time larger ( $\hat{R}_p = 26.8 \times 10^1 \Omega$ ). The detector output is given by

$$V_{AC} = E \frac{R_2}{\hat{R}_p} \quad (22)$$

and many units also have an offset signal, provided by  $R_1$ , so that the detector output is zero when the conductivity is  $40.2 \text{ mS cm}^{-1}$ , nominal, which is also roughly the typical conductivity of seawater. This doubles the useful range of the electronics. Units destined for freshwater and low-salinity environments do not have this offset feature. The output from the synchronous detector is

$$V_{DC} = \frac{2}{\pi} V_{AC} = E \frac{2R_2}{\pi \hat{R}_p}. \quad (23)$$

Using the nominal relationship between probe conductance and accounting for the transformer we have

$$V_{DC} = \frac{2}{\pi} E \left( \frac{\sigma R_2}{30 \times 26800} - \frac{R_2}{R_1} \right). \quad (24)$$

Resistors  $R_1$  and  $R_2$  are usually  $20\text{k}\Omega$ , and using  $E = \sqrt{2}E_{\text{rms}} = 1.56\text{V}$  gives

$$V_{DC} = 24.6 \times 10^{-3} \sigma - 0.99, \quad (25)$$

and re-arranging this gives

$$\sigma = 40.6 V_{DC} + 40.2 \text{ [mS cm}^{-1}\text{]}. \quad (26)$$

This is the nominal relationship between the output voltage from the micro-conductivity board, connected to an SBE7 probe, and the fluid conductivity. The analog-to-digital converter in most instruments has a full-scale span of  $\pm 2.5\text{V}$  spaced over 16 bits. The conductivity in terms of raw digital data is then

$$\sigma = \frac{5}{2^{16}} 40.6 N_C + 40.2 \text{ [mS cm}^{-1}\text{]}. \quad (27)$$

where  $N_C$  is the digital data (in units of counts) produced by the analog-to-digital converter and are the numbers in a raw data file.

### Using Micro-conductivity calibration report

Every micro-conductivity board is “calibrated” by substituting the probe with known resistances (hence, conductances). The entire report is included in the instrument manual. The slope of the voltage-to-conductance graph (Figure 9) can then be used to scale the output in terms of conductivity knowing that the conductance is the inverse of  $268\Omega$  when the fluid conductivity is  $30 \text{ mS cm}^{-1}$ . For example, board SN029 has a slope of  $178 \text{ V S}^{-1}$ , that is,

$$V_{DC} = \frac{178}{R_p} = \frac{178\sigma}{268 \times 30} = 22.1 \times 10^3 \sigma, \text{ or} \quad (28)$$

$$\sigma = 45.2 V_{DC} = \frac{5 \times 45.2}{2^{16}} N_C \text{ [mS cm}^{-1}\text{]}$$

and to this one must add the offset (if any) of  $40.2$ . This provides a better estimate than using the nominal electronics gains but still presumes that the resistance of the SBE7 probe is  $268\Omega$  when the conductivity is  $30 \text{ mS cm}^{-1}$ . The best calibration is provided by simultaneous measurements of conductivity with a high-accuracy sensor, such as the SBE4C, but this is not always available.

If your data indicate that the measured conductivity derived using (28) is significantly in error based upon knowledge of the environmental conductivity, then the probe should be carefully checked for surface contaminants and cleaned with Triton solution, as recommended by Sea-Bird for their SBE4C sensors. This information is available on their web-site. A quick check of the electronics is provided by the dummy micro-conductivity probe supplied with your instrument. With it installed, your readings should be close to zero (if your board has an offset feature), and the derived conductivity is  $\sim 30 \text{ mS cm}^{-1}$ .

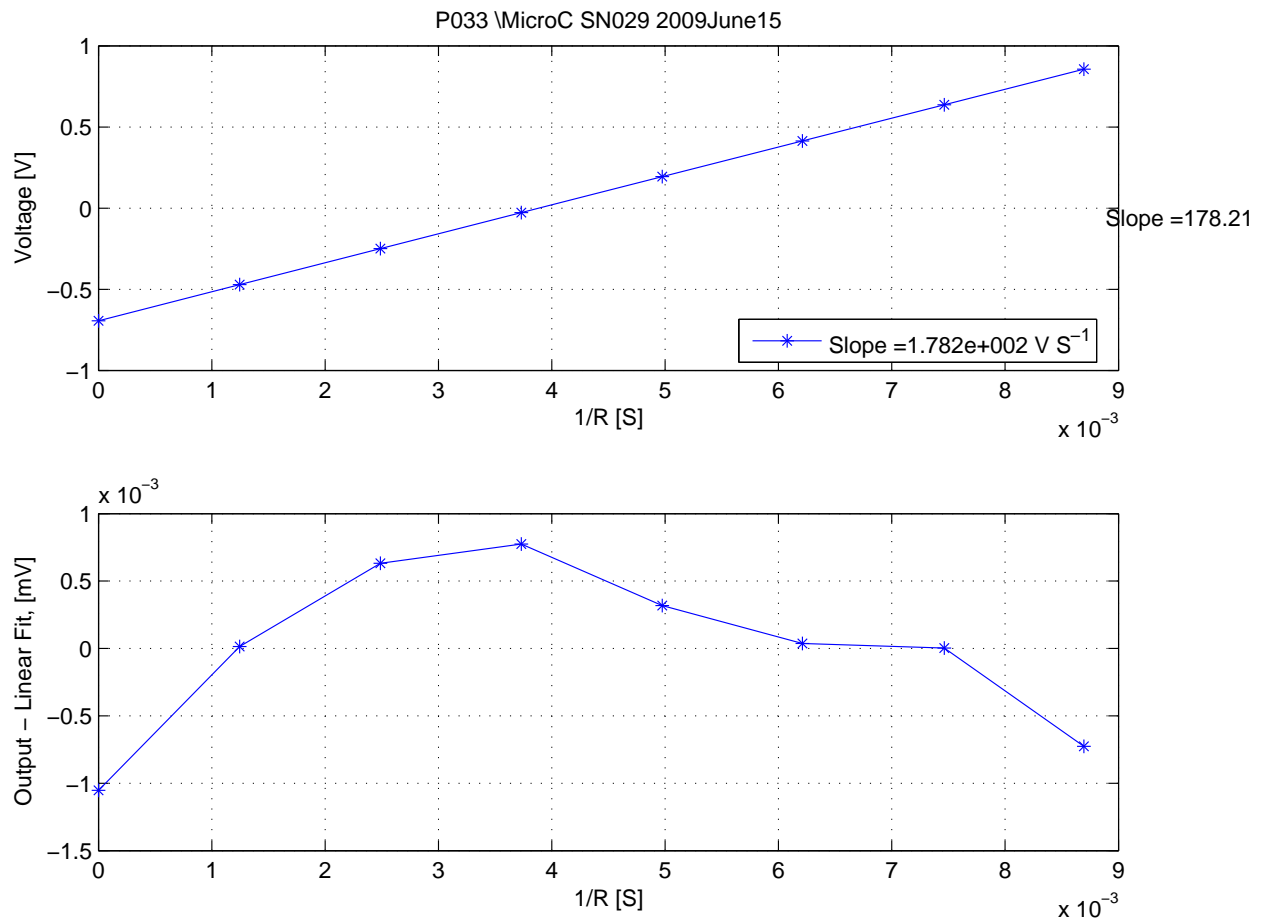


Figure 9. Typical “calibration” of a micro-conductivity board.

### Micro-conductivity De-convolution

The output of the micro-conductivity board is proportional to the conductivity plus its rate-of-change. Use the procedures described in section “Temperature De-convolution” to deconvolve the micro-conductivity signal.

## References

- Mudge, T. and R. G. Lueck, 1994: Digital signal processing to enhance oceanographic observations. *J. Atmos. and Oceanic Technol.*, **11**, 825-836.
- Macoun, P. and R. Lueck, 2004: Modeling the spatial response of the airfoil shear probe using different sized probes. *J. Atmos. and Oceanic Technol.*, **21**, 284-297.
- Osborn, T. R., 1974: Vertical profiling of velocity microstructure. *J. Phys. Oceanogr.*, **4**, 109-115.
- Osborn, T. R. and W. R. Crawford, 1980: An airfoil probe for measuring turbulent velocity fluctuations in water. *Air-Sea Interaction: Instruments and Methods*, F. W. Dobson and R. Davis, Eds., Plenum, 369-386.
- Siddon, T. E. and H. S. Ribner, 1965: An aerofoil probe for measuring the transverse component of turbulence. *J. American Inst. Aeronautics and Astronautics*, **3**, 747-749.

End-of-Document

---